Anisotropic two-gap superconductivity and the absence of a Pauli paramagnetic limit in single-crystalline $LaO_{0.5}F_{0.5}BiS_2$

Y. C. Chan,[1] K. Y. Yip,[1] Y. W. Cheung,[1] Y. T. Chan,[1] Q. Niu,[1] J. Kajitani,[2] R. Higashinaka,[2] T. D. Matsuda,[2] Y. Yanase,[3] Y. Aoki,[2] K. T. Lai,[1] and Swee K. Goh[1,4,*]

[1]*Department of Physics, The Chinese University of Hong Kong, Shatin, New Territories, Hong Kong, China*
[2]*Department of Physics, Tokyo Metropolitan University, Hachioji, Tokyo 192-0397, Japan*
[3]*Department of Physics, Kyoto University, Kyoto 606-8502, Japan*
[4]*Shenzhen Research Institute, The Chinese University of Hong Kong, Shatin, New Territories, Hong Kong, China*

(Received 27 October 2017; revised manuscript received 6 December 2017; published 15 March 2018)

Ambient-pressure-grown $LaO_{0.5}F_{0.5}BiS_2$ with a superconducting transition temperature $T_c \sim 3$ K possesses a highly anisotropic normal state. By a series of electrical resistivity measurements with a magnetic-field direction varying between the crystalline c axis and the ab plane, we present datasets displaying the temperature dependence of the out-of-plane upper critical field $H_{c2}^{\perp}(T)$, the in-plane upper critical field $H_{c2}^{\parallel}(T)$, as well as the angular dependence of H_{c2} at fixed temperatures for ambient-pressure-grown $LaO_{0.5}F_{0.5}BiS_2$ single crystals. The anisotropy of the superconductivity, $H_{c2}^{\parallel}/H_{c2}^{\perp}$, reaches ~16 on approaching 0 K, but it decreases significantly near T_c. A pronounced upward curvature of $H_{c2}^{\parallel}(T)$ is observed near T_c, which we analyze using a two-gap model. Moreover, $H_{c2}^{\parallel}(0)$ is found to exceed the Pauli paramagnetic limit, which can be understood by considering the strong spin-orbit coupling associated with Bi as well as the breaking of the local inversion symmetry at the electronically active BiS_2 bilayers. Hence, $LaO_{0.5}F_{0.5}BiS_2$ with a centrosymmetric lattice structure is a unique platform to explore the physics associated with local parity violation in the bulk crystal.

DOI: 10.1103/PhysRevB.97.104509

I. INTRODUCTION

The recent discovery of superconductivity in compounds containing BiS_2 layers [1–3] has quickly inspired comparisons with other well-known layered superconductors, such as cuprates [4,5] and Fe-based systems [6,7]. The structural similarity stems from the fact that the BiS_2 layers are separated from each other by some block layers, which can be chemically manipulated to induce superconductivity. For instance, the insulating parent compound $ROBiS_2$ (R is a rare-earth element) can be made superconducting through the partial substitution of O by F [8–10]. This partial substitution introduces extra electrons onto the BiS_2 layers, making the system more metallic before the realization of a superconducting ground state at low temperatures. Additionally, the superconducting state can be induced via a partial substitution of R with tetravalent elements such as Th, Hf, Zr, or Ti [11]. Given the flexibility of chemically manipulating the block layers to induce superconductivity, more BiS_2-based superconductors with a variety of block layers can be expected.

$LaO_{1-x}F_xBiS_2$ is one of the most heavily studied BiS_2-based series [12–17]. With an increasing F concentration x, superconductivity appears at $x \geqslant 0.2$, and the superconducting transition temperature (T_c) reaches a maximum of ~3 K at $x = 0.5$ [9,12]. With the application of an external pressure of around 1 GPa, T_c of $LaO_{0.5}F_{0.5}BiS_2$ can be rapidly enhanced to ~10 K [13,18,19]. Interestingly, $LaO_{0.5}F_{0.5}BiS_2$ synthesized under high pressure can superconduct at 10.5 K even at ambient pressure [9,12,13], which represents the highest T_c among all BiS_2-based superconductors discovered thus far. To distinguish between two variants of $LaO_{0.5}F_{0.5}BiS_2$, we denote the ambient-pressure-grown and high-pressure-annealed samples as AP − $LaO_{0.5}F_{0.5}BiS_2$ and HP − $LaO_{0.5}F_{0.5}BiS_2$, respectively.

The layered nature of BiS_2-based systems naturally raises a question concerning the anisotropy of the electronic and superconducting properties. Band-structure calculations show that the Fermi surface is cylindrical with a negligible k_z dependence and a strong nesting at $(\pi,\pi,0)$ [20–22], indicating a highly anisotropic electronic structure. To extract the anisotropy of the superconductivity, upper critical fields (H_{c2}) under varying temperatures and applied magnetic-field directions are powerful probes. For HP − $LaO_{0.5}F_{0.5}BiS_2$, the upper critical field anisotropy was inferred by analyzing the temperature derivative of the electrical resistivity of polycrystals, resulting in an anisotropy factor γ of 7.4 [23], where $\gamma = H_{c2}^{\parallel}/H_{c2}^{\perp}$, with $H_{c2}^{\parallel}$ ($H_{c2}^{\perp}$) being the in-plane (out-of-plane) upper critical field. For AP − $LaO_{0.5}F_{0.5}BiS_2$, while single crystals have been available for quite some time, the construction of the temperature-field phase diagrams with different field directions is surprisingly absent.

In this article, we present datasets showing H_{c2} of AP − $LaO_{0.5}F_{0.5}BiS_2$ measured at different field directions, constructed by measuring the electrical resistivity of single crystals. Our data indicate that the superconductivity is highly anisotropic. Furthermore, $H_{c2}^{\parallel}(T)$ exhibits a pronounced upward curvature near T_c, and the $H_{c2}^{\parallel}(0)$ is enhanced well beyond the Pauli paramagnetic limit H_p.

*skgoh@phy.cuhk.edu.hk

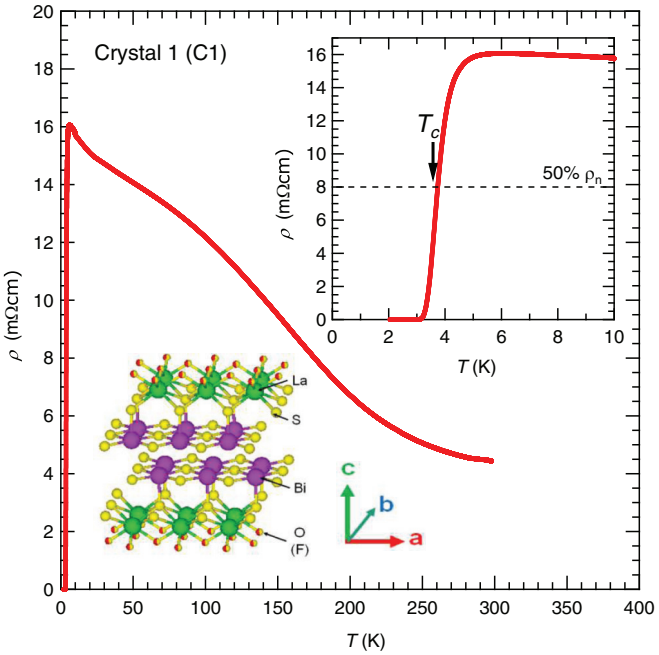

FIG. 1. Temperature dependence of resistivity $\rho(T)$ at ambient pressure without a magnetic field for crystal 1. Top inset: the enlarged resistivity curve near the superconducting transition, with the arrow indicating the T_c, defined as 50% of the normal state resistivity ρ_n. Bottom inset: the crystal structure of $LaO_{0.5}F_{0.5}BiS_2$ with a space group of $P4/nmm$.

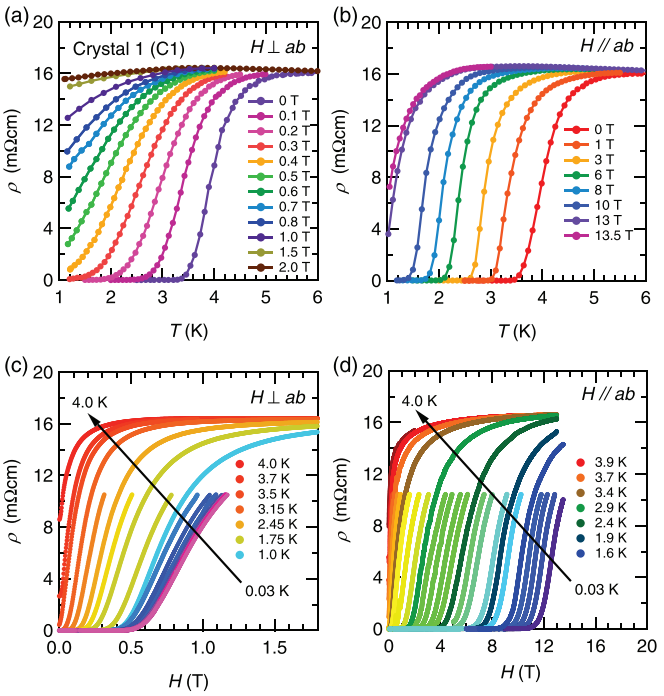

FIG. 2. Temperature dependence of resistivity $\rho(T)$ for crystal 1 under various magnetic fields with (a) $H \perp ab$ and (b) $H \parallel ab$. Field dependence of resistivity $\rho(H)$ at different temperatures with (c) $H \perp ab$ and (d) $H \parallel ab$. The black arrow indicates increasing temperatures. Representative curves covering a longer field range are labeled in the legend.

II. EXPERIMENT

Single crystals of $LaO_{0.5}F_{0.5}BiS_2$ were grown by the CsCl flux method using stoichiometrically mixed starting materials consisting of La_2S_3 (99.9%), Bi_2O_3 (99.999%), and BiF_3 (99.99%) powders, as well as Bi (99.99%) and Bi_2S_3 (99.999%) grains. They were homogenized with the flux medium CsCl (99.9%) and were then sealed in a quartz tube under a vacuum of 1×10^{-3} Pa. The ampoule was annealed at 900 °C for 12 h, followed by a slow cooling to 500 °C at a rate of 2.4 °C/h. After the heat treatment, the flux was removed by H_2O to extract single crystals. Single-crystal and powder x-ray analyses have shown that the crystal structure belongs to the space group $P4/nmm$ (cf. Fig. 1) and the lattice parameters are $a = 4.0585$ Å and $c = 13.324$ Å, which is consistent with previous reports [12]. Assuming Vegard's law [17], the value of c indicates $x = 0.502 \pm 0.029$. The temperature dependence of electrical resistivity $\rho(T)$ was measured using a standard four-probe technique with current flowing in the ab plane. The electrical contacts were made with gold wires glued on a freshly cleaved surface of the sample by silver paste (Dupont 6838). Crystal 1 (C1) was measured down to 30 mK using a dilution fridge (BlueFors Cryogenics) equipped with a 14 T magnet, whereas crystal 2 (C2) was studied using a rotator in a Physical Property Measurement System (Quantum Design) down to 2.0 K.

III. RESULTS AND DISCUSSION

Figure 1 shows $\rho(T)$ for C1 from 300 to 2 K at ambient pressure without a magnetic field. The $\rho(T)$ curve exhibits a semiconducting-like behavior, which broadly resembles that of polycrystalline samples [13,18,19,24], except for a convex curvature from ~15 to 200 K. The convex curvature could be related to the discovery of weak superlattice reflections at low temperatures by single-crystal x-ray diffraction [25]. The top inset shows the enlarged $\rho(T)$ curve from 2 to 10 K, featuring a sharp superconducting transition with the onset temperature ~5 K. For the quantitative analysis of the superconductivity, we adopt the "50% criterion," as indicated by the arrow in the top inset of Fig. 1, by defining T_c (H_{c2}) as the temperature (field) at which the resistivity is 50% of the normal state value ρ_n. With this criterion, T_c of C1 is 3.7 K.

Figures 2(a) and 2(b) show $\rho(T)$ for C1 under various magnetic fields with $H \perp ab$ and $H \parallel ab$, respectively. For $H \perp ab$, T_c is greatly suppressed with an increasing magnetic field. On the contrary, for $H \parallel ab$, T_c is significantly more robust against the applied field, indicating a large anisotropy factor γ for $LaO_{0.5}F_{0.5}BiS_2$. At low temperatures, the superconducting transition becomes significantly broader for $H \perp ab$. The broadening can be quantified by $\Delta T_c/T_c = [T_c(90\%\rho_n) - T_c(10\%\rho_n)]/T_c(50\%\rho_n)$. For $H \parallel ab$, $\Delta T_c/T_c$ merely increases from ~0.26 at T_c to 0.46 at $0.44T_c$. However, for $H \perp ab$, $\Delta T_c/T_c$ already reaches 0.82 at $0.56T_c$. These in-field behaviors could be due to the poor pinning of pancake vortices in this anisotropic, two-dimensional superconductor. This scenario is plausible, since $\xi_\perp$ (see below) is less than the lattice constant c.

Figures 2(c) and 2(d) display the field dependence of electrical resistivity $\rho(H)$ at different temperatures from 4.0 K

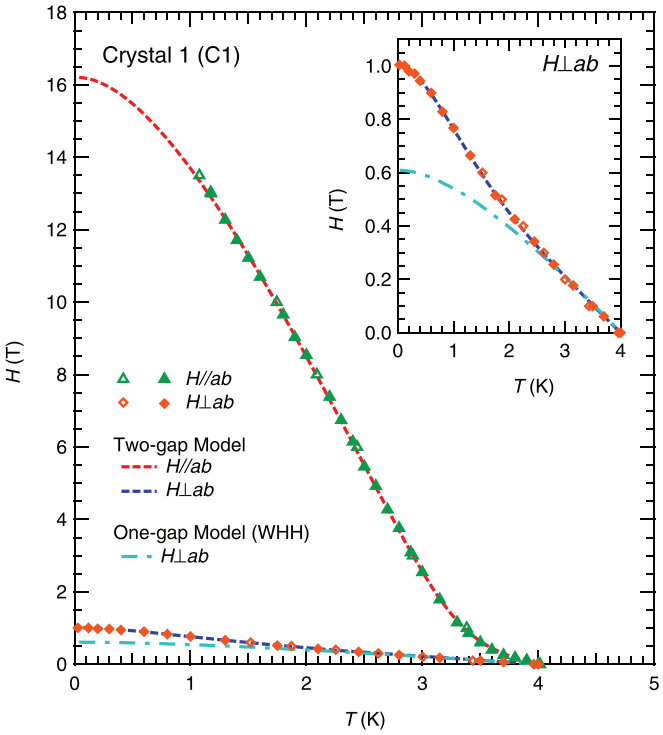

FIG. 3. Temperature dependence of H_{c2} with $H \parallel ab$ and $H \perp ab$ for crystal 1. Experimental data, shown in symbols, are fitted with the two-gap model (dashed line) and the Werthamer-Helfand-Hohenberg (WHH) theory (dash-dotted line). Inset: the enlargement of the low-field region for a clearer view of $H_{c2}^{\perp}(T)$.

down to ~30 mK with $H \perp ab$ and $H \parallel ab$, respectively. With increasing H for $H \perp ab$, $\rho(H)$ increases and, at 4.0 and 1.0 K, saturates at the same field-independent normal state value of 16.0 mΩ cm. This shows that the magnetoresistance does not vary strongly within the field and temperature windows of interest. With $H \parallel ab$, the magnetoresistance is expected to be even weaker. In fact, the weak magnetoresistance is not surprising, given the large residual resistivity of the sample. Hence, we take 16.0 mΩ cm as the universal normal state resistivity for the determination of H_{c2}. Again, H_{c2} determined from $\rho(H)$ is sensitive to the field direction [note the range of field axes in Figs. 2(c) and 2(d)].

From $\rho(T)$ and $\rho(H)$, we construct the H-T phase diagram for $H \parallel ab$ and $H \perp ab$, as displayed in Fig. 3. The critical values obtained from both temperature sweeps (open symbols) and field sweeps (closed symbols) overlap smoothly, exhibiting excellent agreement with each other. From these data, $\xi_{\parallel}$ and $\xi_{\perp}$ can be calculated by using $H_{c2}^{\perp} = \frac{\phi_0}{2\pi\xi_{\parallel}^2}$ and $H_{c2}^{\parallel} = \frac{\phi_0}{2\pi\xi_{\parallel}\xi_{\perp}}$, resulting in $\xi_{\parallel} \sim 21.7$ nm and $\xi_{\perp} \sim 1.13$ nm at 1 K. Our single-crystal data further reveal two interesting behaviors that have not been reported in polycrystalline $LaO_{0.5}F_{0.5}BiS_2$ studies [16,18,26]. First, $H_{c2}^{\parallel}(T)$ becomes unexpectedly high when approaching 0 K. Below 2 K, it exceeds the Pauli limited field $H_p(0)\,[\mathrm{T}] = 1.84T_c\,[\mathrm{K}] \approx 7.36$ T for weakly coupled BCS superconductors [27,28]. Second, a pronounced upward curvature of $H_{c2}^{\parallel}(T)$ near T_c is observed. These features are unambiguously not compatible with the one-gap Werthamer-Helfand-Hohenberg (WHH) theory [29]. On the other hand, $H_{c2}^{\perp}(T)$ is much smaller and shows an upward curvature near 2 K (see the inset of Fig. 3). We have simulated the temperature dependence of H_{c2} using the WHH theory (dash-dotted line), and the mismatch between the data and the simulation clearly implies that the WHH theory is also not applicable to $H_{c2}^{\perp}(T)$.

Muon spin relaxation measurements on $AP-LaO_{0.5}F_{0.5}BiS_2$ suggest the possibility of the two-gap superconductivity [30]. In addition, scanning tunneling spectroscopy data on $NdO_{0.5}F_{0.5}BiS_2$ reveal the existence of two superconducting gaps [31]. It has been pointed out that $H_{c2}(T)$ can be rather unconventional in the presence of multiple superconducting gaps, as discussed in MgB_2 and several iron-based superconductors [32–34]. Inspired by these works, we apply the two-gap model [35] to analyze the temperature dependence of H_{c2} for $LaO_{0.5}F_{0.5}BiS_2$. Within the two-gap model in the dirty limit, $H_{c2}(T)$ is implicitly described by

$$a_0[\ln t + U(h)][\ln t + U(\eta h)] + a_2[\ln t + U(\eta h)] + a_1[\ln t + U(h)] = 0 \qquad (1)$$

with $a_1 = 1 + (\lambda_{11} - \lambda_{22})/[(\lambda_{11} - \lambda_{22})^2 + 4\lambda_{12}\lambda_{21}]^{1/2}$, $a_2 = 1 - (\lambda_{11} - \lambda_{22})/[(\lambda_{11} - \lambda_{22})^2 + 4\lambda_{12}\lambda_{21}]^{1/2}$, $a_0 = 2(\lambda_{11}\lambda_{22} - \lambda_{12}\lambda_{21})/[(\lambda_{11} - \lambda_{22})^2 + 4\lambda_{12}\lambda_{21}]^{1/2}$, $t = T/T_c$, $h = D_1 H_{c2}/2\phi_0 T$, $\eta = D_2/D_1$, and $U(x) = \psi(x + 0.5) - \psi(0.5)$. λ_{11} and λ_{22} are the intraband superconducting coupling constants, while λ_{12} and λ_{21} describe the interband coupling. ϕ_0 is the magnetic flux quantum. D_1 (D_2) is the diffusion coefficient of band 1 (band 2) (band 1 is defined as the band with the stronger coupling constant). $\psi(x)$ is the digamma function. The results of the fit are illustrated as the dashed lines in Fig. 3, which clearly describe the experimental data nicely. Based on this model, $H_{c2}^{\parallel}(0)$ is estimated to be 16.2 T. Hence, γ is as high as 16 as $T \to 0$.

The diffusion coefficient D_2 extracted from the analysis is larger than D_1 for both $H \perp ab$ and $H \parallel ab$. This explains the upward curvature of H_{c2} for both field orientations. The smaller value for D_1 implies that band 1 is dirtier [36], which could be the main contributing factor to the large enhancement of H_{c2} at low temperatures. Indeed, previous studies [37,38] have already demonstrated a significant enhancement of H_{c2} by adding impurities and/or introducing defects to the superconducting systems.

Whether or not our sample is in the dirty limit can be evaluated by comparing $\xi_{\parallel}$ with the Pippard coherence length ξ_0. Assuming a single cylindrical Fermi surface, the Fermi wave vector can be written as $k_F = \sqrt{2\pi nc} \simeq 1.02 \times 10^9$ m^{-1}, where c is the lattice constant and $n \simeq 1.24 \times 10^{20}$ cm^{-3} at 10 K [39]. The normal state resistivity of the sample does not vary much below 10 K (see the top inset of Fig. 1), therefore n is not expected to change drastically at this temperature range. Taking an effective mass $m^*/m_e \approx 0.25$, estimated from Refs. [40,41], and $T_c = 4$ K, we calculate that $\xi_0 = 0.18 \times \frac{\hbar v_F}{k_B T_c} = 0.18 \times \frac{\hbar^2 k_F}{m^* k_B T_c} \simeq 163$ nm. Thus, $\xi_{\parallel}$ is much smaller than ξ_0. The mean free path ℓ can be estimated from $\xi_{\parallel}^{-1} = \xi_0^{-1} + \ell^{-1}$, leading to $\ell \simeq 25$ nm. Hence, the criterion $\ell/\xi_0 \ll 1$ is satisfied even for a crude estimation [42], leading to the conclusion that the system is in the dirty limit.

Although the two-gap model in the dirty limit successfully captures the temperature dependence of both $H_{c2}^{\parallel}$ and $H_{c2}^{\perp}$, the absence of the Pauli limit should be noted: $H_{c2}^{\parallel}(0)$ exceeds the Pauli field by a factor of 2. Because of the large atomic number of Bi, the system has a strong spin-orbit coupling (SOC). A possible mechanism is spin-orbit scattering, in which the electron scattering depends on both its spin and orbital angular momentum in the presence of strong SOC. Theoretical calculations showed that such a spin-orbit scattering can enhance $H_{c2}^{\parallel}(0)$ by up to five times of H_p [43]. Another mechanism is related to the spatial symmetry of the crystal structure. $LaO_{0.5}F_{0.5}BiS_2$ crystallizes in a centrosymmetric space group $P4/nmm$, which possesses a global inversion symmetry. However, upon examining the crystal structure of $LaO_{0.5}F_{0.5}BiS_2$ (Fig. 1), the electronically active BiS_2 bilayers do not possess an inversion symmetry. Such a breaking of the local inversion symmetry can result in a large Rashba-Dresselhaus SOC [40,44–49], which locks the spin directions onto the ab plane. Hence the coupling between the external in-plane field and these spins is reduced, effectively protecting the Cooper pairs from depairing, and consequently the Zeeman effect is suppressed. Therefore, the combined effects from the dirty two-gap case and the strong spin-orbit coupling can explain the huge enhancement of $H_{c2}^{\parallel}(0)$ in $LaO_{0.5}F_{0.5}BiS_2$. In the isostructural compounds $LaO_{0.5}F_{0.5}BiSe_2$ and $LaO_{0.5}F_{0.5}BiSSe$, a similar enhancement of $H_{c2}^{\parallel}$ at low temperatures has also been reported [50–52], which can be understood using the same framework developed for our case. The anisotropy factor γ at the 0 K limit is 13.6 and 32.3 for $LaO_{0.5}F_{0.5}BiSe_2$ and $LaO_{0.5}F_{0.5}BiSSe$, respectively. Note that other contributions to H_{c2} enhancement may be possible, such as strong electron-phonon coupling and localized charge-density waves predicted by band-structure calculations [20,21,53–55]. Further investigations will shed light on this issue.

To further investigate the anisotropic superconductivity in single-crystalline $LaO_{0.5}F_{0.5}BiS_2$, we measured the angular dependence of H_{c2} in crystal 2 (C2) at 2, 2.3, and 2.55 K. Although C2 has a lower T_c of 2.84 K, the H-T phase diagram is similar to C1 discussed earlier, as shown in the top inset of Fig. 4. In the main panel of Fig. 4, the collected $H_{c2}(\theta)$ data of C2 are displayed. H_{c2} is highly sensitive to the field angle, and $H_{c2}(\theta)$ can be reasonably well-described by the two-gap model [35]:

$$H_{c2}(\theta) = \frac{8\phi_o(T_c - T)}{\pi^2[a_1 D_1(\theta) + a_2 D_2(\theta)]} \quad (2)$$

with the angular-dependent diffusivities $D_1(\theta)$ and $D_2(\theta)$:

$$D_m(\theta) = \left[D_m^{(a)2}\cos^2\theta + D_m^{(a)}D_m^{(c)}\sin^2\theta\right]^{1/2},\ m = 1,2, \quad (3)$$

where $D_m^{(a)}$ and $D_m^{(c)}$ are the principal values of the diffusivity tensor in the ab plane and along the c axis, respectively. For this analysis, we also obtain $D_2 > D_1$ for all angles θ, consistent with the analysis of $H_{c2}(T)$ exhibited in the top inset of Fig. 4 and in Fig. 3. For comparison, we also perform an analysis with a one-gap model by setting $a_2 = 0$, $D_2 = 0$, and $a_1 = 2$. The one-gap model, which is equivalent to the anisotropic mass model, gives a slightly poorer description of the data, as evidenced in the dataset at 2.55 K (see the bottom inset of Fig. 4). Therefore, both the angular dependence and the temperature dependence of H_{c2} in $LaO_{0.5}F_{0.5}BiS_2$ are in good agreement with the two-gap model.

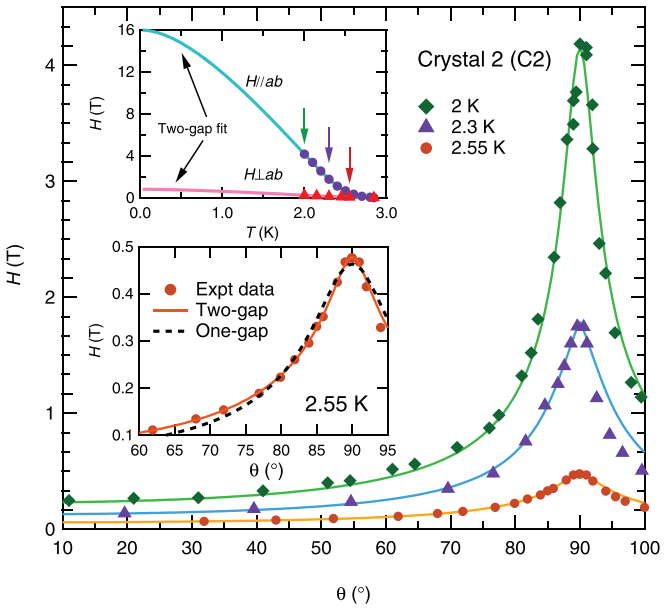

FIG. 4. Angular dependence of H_{c2} for crystal 2 at 2, 2.3, and 2.55 K (solid symbols). The solid lines are the fits using the two-gap model. The angle $\theta = 90^\circ$ (0°) corresponds to $H \parallel ab$ ($H \perp ab$). Top inset: H-T phase diagram constructed for crystal 2, showing a temperature dependence similar to the sample discussed earlier. Arrows indicate the temperatures where angular-dependent studies were conducted. Bottom inset: expanded low-field region for a clearer view of $H_{c2}(\theta)$ at 2.55 K.

Recently, laser-based angle-resolved photoemission spectroscopy (ARPES) on $NdO_{0.71}F_{0.29}BiS_2$ revealed the existence of gap nodes on the same Fermi sheet, giving rise to superconducting gaps of distinct sizes [56]. These gaps could be responsible for the two-gap physics we discussed above. A recent calculation discusses the possibility of having two different gaps on a single Fermi surface sheet, and it shows that the gaps are connected to the variation of orbital mixing along the Fermi surface sheet [57]. However, thermal conductivity [58] and penetration depth [59] measurements on the same Nd-based systems did not detect the existence of the gap nodes. It has been argued that the laser ARPES study probes a much smaller, and hence more homogeneous, region than the other probes. Similar studies on $LaO_{0.5}F_{0.5}BiS_2$, in which we observe strong evidence of two-gap superconductivity, are highly desirable.

IV. CONCLUSIONS

In summary, we have measured both the angular- and temperature-dependent H_{c2} of $LaO_{0.5}F_{0.5}BiS_2$ single crystals. The temperature dependence of H_{c2} at $H \parallel ab$ shows a pronounced upward curvature, and at low temperatures $H_{c2}^{\parallel}$ greatly exceeds the Pauli paramagnetic limit. We employ a dirty-limit two-gap model to describe our data, and we discuss the role of spin-orbit coupling resulting from the breaking of the local inversion symmetry. The angular dependence of H_{c2} can also be described satisfactorily with the two-gap model.

Our data show that $LaO_{0.5}F_{0.5}BiS_2$ is a highly anisotropic two-gap spin-orbit coupled superconductor.

ACKNOWLEDGMENTS

We acknowledge Corentin Morice for discussion. This work was supported by Research Grants Council of Hong Kong (GRF/14301316, GRF/14300117)), CUHK Direct Grants (No. 3132719 and No. 3132720), CUHK Startup (No. 4930048), National Natural Science Foundation of China (No. 11504310), JSPS KAKENHI (JP15H03693, JP15K05178, JP16J05692, JP16K05454, JP15K05164, and JP15H05745), Grant-in-Aid for Scientific Research on Innovative Areas "J-Physics" (JP15H05884), and "Topological Materials Science" (JP16H00991).

Y.C.C. and K.Y.Y. contributed equally to this work.

[1] Y. Mizuguchi, H. Fujihisa, Y. Gotoh, K. Suzuki, H. Usui, K. Kuroki, S. Demura, Y. Takano, H. Izawa, and O. Miura, Phys. Rev. B **86**, 220510 (2012).

[2] S. K. Singh, A. Kumar, B. Gahtori, G. Sharma, S. Patnaik, and V. P. Awana, J. Am. Chem. Soc. **134**, 16504 (2012).

[3] D. Yazici, I. Jeon, B. D. White, and M. B. Maple, Physica C **514**, 218 (2015).

[4] J. G. Bednorz and K. A. Müller, Z. Phys. B **64**, 189 (1986).

[5] M. K. Wu, J. R. Ashburn, C. J. Torng, P. H. Hor, R. L. Meng, L. Gao, Z. J. Huang, Y. Q. Wang, and C. W. Chu, Phys. Rev. Lett. **58**, 908 (1987).

[6] Y. Kamihara, T. Watanabe, M. Hirano, and H. Hosono, J. Am. Chem. Soc. **130**, 3296 (2008).

[7] M. Rotter, M. Tegel, and D. Johrendt, Phys. Rev. Lett. **101**, 107006 (2008).

[8] D. Yazici, K. Huang, B. D. White, A. H. Chang, A. J. Friedman, and M. B. Maple, Philos. Mag. **93**, 673 (2013).

[9] Y. Mizuguchi, T. Hiroi, J. Kajitani, H. Takatsu, H. Kadowaki, and O. Miura, J. Phys. Soc. Jpn. **83**, 053704 (2014).

[10] C. Morice, E. Artacho, S. E. Dutton, H.-J. Kim, and S. S. Saxena, J. Phys.: Condens. Matter **28**, 345504 (2016).

[11] D. Yazici, K. Huang, B. D. White, I. Jeon, V. W. Burnett, A. J. Friedman, I. K. Lum, M. Nallaiyan, S. Spagna, and M. B. Maple, Phys. Rev. B **87**, 174512 (2013).

[12] Y. Mizuguchi, S. Demura, K. Deguchi, Y. Takano, H. Fujihisa, Y. Gotoh, H. Izawa, and O. Miura, J. Phys. Soc. Jpn. **81**, 114725 (2012).

[13] H. Kotegawa, Y. Tomita, H. Tou, H. Izawa, Y. Mizuguchi, O. Miura, S. Demura, K. Deguchi, and Y. Takano, J. Phys. Soc. Jpn. **81**, 103702 (2012).

[14] K. Deguchi, Y. Mizuguchi, S. Demura, H. Hara, T. Watanabe, S. J. Denholme, M. Fujioka, H. Okazaki, T. Ozaki, H. Takeya *et al.*, Europhys. Lett. **101**, 17004 (2013).

[15] J. Lee, M. B. Stone, A. Huq, T. Yildirim, G. Ehlers, Y. Mizuguchi, O. Miura, Y. Takano, K. Deguchi, S. Demura *et al.*, Phys. Rev. B **87**, 205134 (2013).

[16] R. Higashinaka, R. Miyazaki, Y. Mizuguchi, O. Miura, and Y. Aoki, J. Phys. Soc. Jpn. **83**, 075004 (2014).

[17] M. Nagao, Novel Supercond. Mater. **1**, 64 (2015).

[18] R. Jha, H. Kishan, and V. P. S. Awana, J. Phys. Chem. Solids **84**, 17 (2015).

[19] T. Tomita, M. Ebata, H. Soeda, H. Takahashi, H. Fujihisa, Y. Gotoh, Y. Mizuguchi, H. Izawa, O. Miura, S. Demura *et al.*, J. Phys. Soc. Jpn. **83**, 063704 (2014).

[20] X. Wan, H.-C. Ding, S. Y. Savrasov, and C.-G. Duan, Phys. Rev. B **87**, 115124 (2013).

[21] T. Yildirim, Phys. Rev. B **87**, 020506(R) (2013).

[22] H. Usui, K. Suzuki, and K. Kuroki, Phys. Rev. B **86**, 220501 (2012).

[23] Y. Mizuguchi, A. Miyake, K. Akiba, M. Tokunaga, J. Kajitani, and O. Miura, Phys. Rev. B **89**, 174515 (2014).

[24] C. T. Wolowiec, D. Yazici, B. D. White, K. Huang, and M. B. Maple, Phys. Rev. B **88**, 064503 (2013).

[25] J. Kajitani *et al.* (unpublished).

[26] Y. Fang, C. Wolowiec, A. Breindel, D. Yazici, P.-C. Ho, and M. Maple, Supercond. Sci. Technol. **30** 115004 (2017).

[27] A. M. Clogston, Phys. Rev. Lett. **9**, 266 (1962).

[28] B. S. Chandrasekhar, Appl. Phys. Lett. **1**, 7 (1962).

[29] N. R. Werthamer, E. Helfand, and P. C. Hohenberg, Phys. Rev. **147**, 295 (1966).

[30] J. Zhang, K. Huang, Z. F. Ding, D. E. MacLaughlin, O. O. Bernal, P.-C. Ho, C. Tan, X. Liu, D. Yazici, M. B. Maple *et al.*, Phys. Rev. B **94**, 224502 (2016).

[31] J. Liu, D. Fang, Z. Wang, J. Xing, Z. Du, S. Li, X. Zhu, H. Yang, and H.-H. Wen, Europhys. Lett. **106**, 67002 (2014).

[32] X. Xing, W. Zhou, J. Wang, Z. Zhu, Y. Zhang, N. Zhou, B. Qian, X. Xu, and Z. Shi, Sci. Rep. **7**, 45943 (2017).

[33] J. Hänisch, K. Iida, F. Kurth, E. Reich, C. Tarantini, J. Jaroszynski, T. Förster, G. Fuchs, R. Hühne, V. Grinenko *et al.*, Sci. Rep. **5**, 17363 (2015).

[34] F. Hunte, J. Jaroszynski, A. Gurevich, D. C. Larbalestier, R. Jin, A. S. Sefat, M. A. McGuire, B. C. Sales, D. K. Christen, and D. Mandrus, Nature (London) **453**, 903 (2008).

[35] A. Gurevich, Phys. Rev. B **67**, 184515 (2003).

[36] A. Gurevich, Physica C **456**, 160 (2007).

[37] T. P. Orlando, E. J. McNiff, S. Foner, and M. R. Beasley, Phys. Rev. B **19**, 4545 (1979).

[38] C. Tarantini, A. Gurevich, J. Jaroszynski, F. Balakirev, E. Bellingeri, I. Pallecchi, C. Ferdeghini, B. Shen, H. H. Wen, and D. C. Larbalestier, Phys. Rev. B **84**, 184522 (2011).

[39] V. P. S. Awana, A. Kumar, R. Jha, S. K. Singh, A. Pal, Shruti, J. Saha, and S. Patnaik, Solid State Commun. **157**, 21 (2013).

[40] S.-L. Wu, K. Sumida, K. Miyamoto, K. Taguchi, T. Yoshikawa, A. Kimura, Y. Ueda, M. Arita, M. Nagao, S. Watauchi, I. Tanaka, and T. Okuda, Nat. Commun. **8**, 1919 (2017).

[41] T. Sugimoto, D. Ootsuki, C. Morice, E. Artacho, S. S. Saxena, E. F. Schwier, M. Zheng, Y. Kojima, H. Iwasawa, K. Shimada *et al.*, Phys. Rev. B **92**, 041113 (2015).

[42] Direct estimation of the mean free path using a single-band Drude model and the measured resistivity value lead to $\ell_\rho \simeq 0.34$ nm. This value is much smaller than ℓ estimated from ξ_0 and $\xi_\parallel$. Such a small ℓ_ρ, even slightly smaller than the lattice constant a, is puzzling. The small ℓ_ρ could come from an overestimation of the effective sample thickness, due to the fact that $LaO_{0.5}F_{0.5}BiS_2$ is a highly two-dimensional material, and hence the transport current only flows in the top few layers. Furthermore, the estimation assumes a single, strictly two-dimensional Fermi surface and the absence of any Fermi

surface gapping (e.g., due to charge order). A more realistic estimation could change the values of ℓ_ρ, but is unlikely to affect the conclusion that both ℓ and ℓ_ρ are much smaller than ξ_0.

[43] R. A. Klemm, A. Luther, and M. R. Beasley, Phys. Rev. B **12**, 877 (1975).

[44] M. H. Fischer, F. Loder, and M. Sigrist, Phys. Rev. B **84**, 184533 (2011).

[45] D. Maruyama, M. Sigrist, and Y. Yanase, J. Phys. Soc. Jpn. **81**, 034702 (2012).

[46] A. D. Caviglia, M. Gabay, S. Gariglio, N. Reyren, C. Cancellieri, and J.-M. Triscone, Phys. Rev. Lett. **104**, 126803 (2010).

[47] S. K. Goh, Y. Mizukami, H. Shishido, D. Watanabe, S. Yasumoto, M. Shimozawa, M. Yamashita, T. Terashima, Y. Yanase, T. Shibauchi *et al.*, Phys. Rev. Lett. **109**, 157006 (2012).

[48] M. Shimozawa, S. K. Goh, R. Endo, R. Kobayashi, T. Watashige, Y. Mizukami, H. Ikeda, H. Shishido, Y. Yanase, T. Terashima *et al.*, Phys. Rev. Lett. **112**, 156404 (2014).

[49] X. Zhang, Q. Liu, J.-W. Luo, A. J. Freeman, and A. Zunger, Nat. Phys. **10**, 387 (2014).

[50] J. Shao, Z. Liu, X. Yao, L. Zhang, L. Pi, S. Tan, C. Zhang, and Y. Zhang, Europhys. Lett. **107**, 37006 (2014).

[51] N. Kase, Y. Terui, T. Nakano, and N. Takeda, Phys. Rev. B **96**, 214506 (2017).

[52] Y. Terui, N. Kase, T. Nakano, and N. Takeda, J. Phys. Conf. Ser. **871**, 012005 (2017).

[53] B. Li, Z. W. Xing, and G. Q. Huang, Europhys. Lett. **101**, 47002 (2013).

[54] M. Schossmann and J. P. Carbotte, Phys. Rev. B **39**, 4210 (1989).

[55] C. Morice, R. Akashi, T. Koretsune, S. S. Saxena, and R. Arita, Phys. Rev. B **95**, 180505 (2017).

[56] Y. Ota, K. Okazaki, H. Q. Yamamoto, T. Yamamoto, S. Watanabe, C. Chen, M. Nagao, S. Watauchi, I. Tanaka, Y. Takano *et al.*, Phys. Rev. Lett. **118**, 167002 (2017).

[57] M. A. Griffith, T. O. Puel, M. A. Continentino, and G. B. Martins, J. Phys.: Condens. Matter **29**, 305601 (2017).

[58] T. Yamashita, Y. Tokiwa, D. Terazawa, M. Nagao, S. Watauchi, I. Tanaka, T. Terashima, and Y. Matsuda, J. Phys. Soc. Jpn. **85**, 073707 (2016).

[59] L. Jiao, Z. Weng, J. Liu, J. Zhang, G. Pang, C. Guo, F. Gao, X. Zhu, H.-H. Wen, and H. Q. Yuan, J. Phys.: Condens. Matter **27**, 225701 (2015).